

Direct reconstruction of pp elastic scattering amplitudes and phase shift analyses at fixed energies from 1.80 to 2.70 GeV

J. Bystrický¹, C. Lechanoine-LeLuc², F. Lehar¹

¹ DAPNIA/SPP, CEA/Saclay, F-91191 Gif sur Yvette Cedex, France

² DPNC, University of Geneva, 24, quai Ernest-Ansermet, 1211 Geneva 4, Switzerland

Received: 16 April 1998 / Published online: 2 July 1998

Abstract. The direct reconstruction of the pp elastic-scattering amplitudes and fixed-energy Saclay-Geneva phase shift analyses have been carried out at 1.80, 2.10, 2.40 and 2.70 GeV where complete sets of observables have recently been measured at SATURNE. They provide unique phase shift analysis solutions at 1.80, 2.10 and 2.40 GeV and two solutions at 2.70 GeV. Results of the direct amplitude reconstruction and the Saclay-Geneva phase shift analyses agree at all energies. Results are also compared to the Virginia Polytechnic Institute phase-shift predictions below 2.55 GeV and observed differences are discussed.

1 Introduction

During 1992-1995, pp spin observables have been measured at SATURNE II using a polarized proton beam and a polarized target, in particular at 1.80, 2.10, 2.40 and 2.70 GeV. These data, in conjunction with previous SATURNE II spin observable measurements at the same energies, form complete data sets. In this paper we use these sets to do: 1) a direct reconstruction of scattering amplitudes (DRSA) at a few CM angles, 2) a fixed-energy phase shift analysis (PSA) using the Saclay-Geneva PSA program described in our previous papers [1–3]. These two results are presented and compared.

As well as the previously mentioned SATURNE II data consisting of 10 to 12 different spin observables [4–19], differential cross sections data, measured mainly at ZGS and COSY, were added to the data base. The data base was completed with data measured at nearby energies [20–35]. Data in the forward direction were also included, i.e. spin-independent total cross sections, the spin-dependent total cross section differences $\Delta\sigma_T$ and $\Delta\sigma_L$, the fitted total inelastic cross sections [36] and the real to imaginary amplitude ratios calculated from dispersion relations [37]. The final data base for the PSA consisted of 445, 612, 545 and 303 data points at 1.80, 2.10, 2.40 and 2.70 GeV, respectively. Of course only part of these data were considered in the DRSA as such a reconstruction is performed at a few angular points where the number of different experimental points is sufficient.

The status of the DRSA is as follows: before 1975, the direct reconstruction was only possible for pp elastic scattering at 90 (CM) at a few energies [38]. The first direct reconstruction over a large angular region was carried out using the 0.59 GeV PSI data and was reported in [39]. Similar reconstructions have been subsequently per-

formed using LAMPF data at 0.73 GeV [40], PSI data below 0.59 GeV [41] and LAMPF data at 0.8 GeV [42]. At higher energy, an amplitude analysis was performed [43] using the 6 GeV/ c ANL-ZGS data [44]. Finally the SATURNE II data have also allowed a DRSA analysis at 11 energies between 0.83 and 2.70 GeV [45]. In this later analysis, two solutions were found at a few energies, one in good agreement with PSA: however, the correct solution could not be identified using only the χ^2 values. Measurement of additional parameters has removed this ambiguity: the remaining solution is the one consistent with PSA.

The status of the pp PSA is as follows: below 0.6 GeV complete sets of observables have been measured over a large angular range ensuring unique PSA solutions. At higher energies complete sets of observables do not guarantee unique PSA solution. For instance, in [3] two solutions were found at 1.30 GeV, in the present paper two PSA solutions appear at 2.70 GeV. This is due to a large number of complex phase shifts to fit. To add further constraints we made use of additional information in particular the ratio of the real-to-imaginary parts of the spin-independent forward scattering amplitude [37], the inelastic parts of high orbital momentum phase shifts, as calculated by a dispersion relation method of the Paris group [46–48]. In the present paper, two PSA solutions appear at 2.70 GeV, a unique solution has been found at the three other energies.

The fact that the DRSA and PSA solutions agree shows that our choice of phase shifts is reasonable, but not unique. Some other choice of inelasticities might also have resulted in satisfactory solutions.

In Sect. 2, the nucleon-nucleon formalism necessary for the PSA and DRSA is described. The complementarity of the two analysis methods is discussed in Sect. 3. Section 4 gives details about the data base used and the theoretical

Table 1. Data sets of observables used in PSA at four energies. The “pure” observables are given in Table 1a. The observable combinations, calculated and fitted data, total number of points and χ^2 values per degree of freedom (DF) obtained in PSA are listed in Table 1b

Observables	1.80 GeV		2.10 GeV		2.40 GeV		2.70 GeV	
	Ref.	Points	Ref.	Points	Ref.	Points	Ref.	Points
σ_{0tot}	[20]	1	[20]	1	[20]	2	[20]	1
σ_{1tot}	[5,21,22]	3	[5]	1	[5]	1	[22]	1
$\Delta\sigma_L$	[4,23]	2	[24]	1	[24,31]	2	[4,24]	2
$d\sigma/d\Omega$	[26,27,28,32]	99	[26,28,29,32]	92	[26,28,30,32]	112	[26,28,31]	79
A_{oono}, A_{oono}	[6,19,33]	79	[6,17,19]	123	[6,15,17,19,34]	193	[6,19,34]	72
A_{oonn}	[7,19]	55	[7,19]	84	[7,19]	110	[7,19]	62
A_{ookk}	[8,9]	55	[8,9,35]	99	[8,9,35]	49	[8,35]	38
A_{oosk}	[9,10,16]	48	[9,10,16]	59	[9,10]	25	[9,10,16]	18
D_{onon}	[12,13,16]	14	[12,13,16,18]	27	[12,18]	13	[12,18]	5
K_{onno}	[12,16]	9	[12,16,18]	21	[12,18]	12	[12,18]	5
$D_{os''ok}$	[11,14,16]	18	[11,14,16]	20	[11,14]	7	[11,14]	5
$K_{os''ko}$	[11]	8	[11]	9	[11]	4	[11]	3
$K_{os''so}$	[14,16]	8	[16]	3	[14]	1		0
N_{onkk}	[11]	4	[11]	10	[11]	1		0
N_{onsk}	[16]	3	[11]	3		0		0
$N_{os''sn}$	[16]	3	[11]	3		0		0
$N_{os''nk}$	[14]	3		0	[14]	1	[14]	1

Combinations of Observables	1.80 GeV Points	2.10 GeV Points	2.40 GeV Points	2.70 GeV Points	Ref.
$K_{onno}, K_{ok''so}$	4	0	1	1	[14]
$N_{onsk}, N_{ok''nk}$	0	0	1	1	[14]
$K_{onno}, K_{ok''so}, N_{onsk}, N_{ok''nk}$	6	18	3	2	[14]
$N_{onkk}, K_{ok''ko}$	6	0	3	3	[11]
$N_{os''nk}, K_{os''so}$	5	18	3	2	[14]
$N_{os''kn}, N_{os''sn}, N_{ok''kn}$	6	9	0	0	[13]
$K_{os''ko}, K_{os''so}, K_{ok''ko}$	4	9	0	0	[13]
$\sigma_{tot}(\text{inel.}) - \text{fitted}$	1	1	1	1	[36]
$\Re e(a+b)/\Im m(a+b)$ (calc.)	1	1	1	1	[42]
Total points (Tables 1a and 1b)	445	612	545	303	
χ^2/DF	1.10	1.16	1.07	0.95 A 0.92 B	

input to the PSA. Section 5 describes the minimization procedure for the two methods. Results are presented and discussed in Sect. 6.

2 Scattering matrix and observables

Assuming parity conservation, time reversal and isospin invariance, the scattering matrix is written in terms of complex amplitudes a, b, c, d and e as [49]

$$M(\mathbf{k}_f, \mathbf{k}_i) = \frac{1}{2} [(a+b) + (a-b)(\sigma_1, \mathbf{n})(\sigma_2, \mathbf{n}) + (c+d)(\sigma_1, \mathbf{m})(\sigma_2, \mathbf{m}) + (c-d)(\sigma_1, \boldsymbol{\ell})(\sigma_2, \boldsymbol{\ell}) + e(\sigma_1 + \sigma_2, \mathbf{n})] \quad (2.1)$$

where σ_1 and σ_2 are the Pauli 2x2 matrices, \mathbf{k}_i and \mathbf{k}_f are the unit vectors in the direction of the incident and scattered particles, respectively, and

$$\mathbf{n} = \frac{[\mathbf{k}_i \times \mathbf{k}_f]}{|\mathbf{k}_i \times \mathbf{k}_f|}, \quad \mathbf{m} = \frac{\mathbf{k}_f - \mathbf{k}_i}{|\mathbf{k}_f - \mathbf{k}_i|}, \quad \boldsymbol{\ell} = \frac{\mathbf{k}_f + \mathbf{k}_i}{|\mathbf{k}_f + \mathbf{k}_i|}. \quad (2.2)$$

The subscripts of an observable X_{srbt} refer to the polarization states of the scattered, recoil, beam and target particles, respectively. For the so-called “pure experiments”, the polarizations of the incident and target particles in the laboratory system are oriented along the basis unit vectors $\mathbf{k}, \mathbf{n}, \mathbf{s} = [\mathbf{n} \times \mathbf{k}]$. In our energy region only the recoil proton polarization was analyzed in the second scattering. The base vectors are in the directions \mathbf{k}^*, \mathbf{n} ,

Table 2. Phase shifts and mixing parameters at four energies. The values shown without errors were fixed

T_{kin} (GeV)	Real Parts of Phase Shifts (deg)				
	Imaginary Parts of Phase Shifts (deg)				
	1S_0	3P_0	3P_1	3P_2	ϵ_2
1.80	-65.27 ± 3.67 $+5.71 \pm 2.45$	-61.72 ± 1.01 0.0	-69.75 ± 2.51 $+9.52 \pm 1.75$	-10.40 ± 2.33 $+27.10 \pm 1.34$	-1.12 ± 0.76
2.10	-58.46 ± 1.59 $+0.89 \pm 1.36$	-57.16 ± 0.88 0.0	-61.22 ± 1.14 $+8.53 \pm 0.85$	-7.40 ± 1.48 $+28.33 \pm 1.43$	-0.20 ± 0.55
2.40	-63.89 ± 3.83 $+10.51 \pm 3.81$	-57.78 ± 0.77 0.0	-63.94 ± 1.53 $+16.84 \pm 1.60$	-34.70 ± 3.12 $+34.87 \pm 1.86$	-2.09 ± 0.65
2.70A	-62.23 ± 4.41 $+0.76 \pm 3.50$	-51.63 ± 2.87 0.0	-46.26 ± 1.91 $+0.53 \pm 1.06$	-32.20 ± 5.64 $+24.36 \pm 2.34$	$+0.13 \pm 1.04$
2.70B	-59.43 ± 7.23 $+0.87 \pm 4.44$	-72.31 ± 9.46 $+20.22 \pm 7.37$	-62.63 ± 3.09 $+15.87 \pm 2.89$	-49.59 ± 5.02 $+49.48 \pm 7.56$	-1.48 ± 1.72
	1D_2	3F_2	3F_3	3F_4	ϵ_4
1.80	-20.23 ± 0.72 $+14.45 \pm 1.56$	-22.83 ± 1.38 $+12.13 \pm 0.86$	-18.75 ± 0.80 $+10.28 \pm 0.63$	$+4.74 \pm 0.46$ $+8.28 \pm 0.63$	-1.12 ± 0.50
2.10	-24.97 ± 0.39 $+12.12 \pm 1.02$	-26.12 ± 1.10 $+16.03 \pm 0.97$	-18.92 ± 0.50 $+10.70 \pm 0.41$	$+0.40 \pm 0.41$ $+10.70 \pm 0.44$	-0.91 ± 0.36
2.40	-27.93 ± 1.10 $+15.16 \pm 1.69$	-18.76 ± 1.41 $+12.36 \pm 0.67$	-23.53 ± 1.01 $+9.28 \pm 0.71$	-0.74 ± 0.79 $+14.80 \pm 1.07$	-1.70 ± 0.40
2.70A	-30.06 ± 0.96 $+20.04 \pm 2.32$	-20.81 ± 3.15 $+13.68 \pm 1.49$	-18.78 ± 2.06 $+21.32 \pm 1.57$	-8.03 ± 1.43 16.70 ± 1.24	-3.01 ± 0.46
2.70B	-28.27 ± 0.93 $+16.70 \pm 2.00$	-9.635 ± 1.30 $+11.94 \pm 3.76$	-19.23 ± 1.97 $+14.53 \pm 1.59$	-14.12 ± 1.90 $+24.53 \pm 1.89$	-2.60 ± 0.85
	1G_4	3H_4	3H_5	3H_6	ϵ_6
1.80	-1.85 ± 0.51 $+7.60 \pm 0.18$	-4.26 ± 0.68 $+5.46 \pm 0.40$	-4.02 ± 0.36 $+3.95 \pm 0.30$	$+3.45 \pm 0.29$ $+2.09 \pm 0.25$	-1.41 ± 0.25
2.10	-4.95 ± 0.39 $+9.35 \pm 0.22$	-7.45 ± 0.47 $+6.12 \pm 0.41$	-4.53 ± 0.26 $+6.01 \pm 0.27$	$+2.93 \pm 0.18$ $+4.12 \pm 0.23$	-2.35 ± 0.18
2.40	-7.59 ± 0.60 $+10.01 \pm 0.33$	-5.19 ± 0.93 $+6.89 \pm 0.60$	-6.06 ± 0.31 $+6.34 \pm 0.41$	$+2.14 \pm 0.31$ $+5.21 \pm 0.38$	-2.06
2.70A	-8.87 ± 0.88 $+9.55 \pm 0.75$	-2.19 ± 0.73 $+4.29 \pm 1.05$	-6.69 ± 0.45 $+8.69 \pm 0.73$	$+1.91 \pm 0.56$ $+9.39$	-2.12
2.70B	-8.31 ± 0.63 $+10.39 \pm 0.57$	-3.80 ± 0.92 $+0.44 \pm 0.88$	-7.67 ± 0.89 $+7.01 \pm 0.32$	-0.58 ± 0.85 $+9.39$	-2.12
	1I_6	3J_6	3J_7	3J_8	ϵ_8
1.80	$+2.30 \pm 0.33$ $+2.80 \pm 0.27$	$+0.37 \pm 0.31$ $+0.81$	-2.17 $+1.74$	$+0.98 \pm 0.10$ $+0.24$ fixed	-1.04
2.10	$+0.89 \pm 0.29$ $+3.66 \pm 0.18$	-0.20 ± 0.25 $+1.05$	-2.32 $+2.50$	$+1.28 \pm 0.10$ $+0.59$	-1.11
2.40	-0.05 ± 0.44 $+2.61 \pm 0.27$	-2.09 ± 0.29 $+1.30$	-2.45 $+2.63$	$+2.72 \pm 0.13$ $+1.18$	-1.16
2.70A	$+0.06 \pm 0.39$ $+4.28 \pm 0.46$	$+1.12 \pm 0.69$ $+2.91 \pm 0.59$	-2.56 $+3.06$	$+1.47 \pm 0.46$ $+1.99$	-1.20
2.70B	$+0.35 \pm 0.44$ $+4.74 \pm 0.57$	$+0.29 \pm 0.68$ $+1.70 \pm 0.31$	-2.56 $+3.06$	$+0.31 \pm 0.36$ $+1.99$	-1.20

Table 2. (continued)

T_{kin} (GeV)	Real Parts of Phase Shifts (deg)						
	Imaginary Parts of Phase Shifts (deg)			All phase shifts are fixed			
	1K_8	3L_8	3L_9	$^3L_{10}$	ϵ_{10}	$^1M_{10}$	$^3N_{10}$
1.80	+0.50	+0.48	-1.19				
	+0.79	+0.24	+0.47				
2.10	+0.50	+0.54	-1.29				
	+1.07	+0.34	+0.65				
2.40	+0.50	+0.59	-1.38	+1.55	-0.71	+0.36	+0.32
	+1.35	+0.88	+0.82	+1.55		+0.45	+0.16
2.70AB	+0.50	+0.63	-1.46	+0.42	-0.75	+0.36	+0.35
	+1.64	+1.10	+0.98	+0.47		+0.57	+0.21

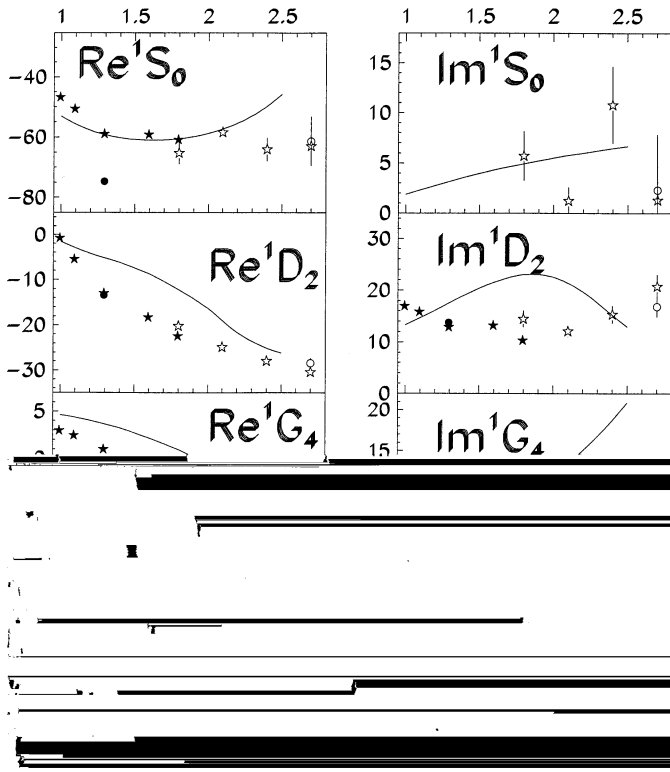


Fig. 1. Phase shift analyses results: Real and imaginary parts of 1S_0 , 1D_2 , 1G_4 and 1I_6 phase shifts in degrees. Open stars denote the present results and the solution 2.70A, open circles correspond to 2.70B. Black stars and black dots are the results from [3] (two solutions at 1.30 GeV were found). Solid lines are the VPI PSA [66], dashed lines are the OPE phase shifts

$\mathbf{s} = [\mathbf{n} \times \mathbf{k}]$, where the unit vector \mathbf{k} is oriented along the direction of the recoil particle momentum.

The pp scattering matrix contains the isotriplet (M_1) matrix only. Ignoring the electromagnetic interactions, the symmetry relations with respect to 90° CM for different amplitudes are given in [49]. Taking into account fundamental conservation laws, we express the contributing observables in terms of five scattering amplitudes a , b , c , d , and e from (2.1).

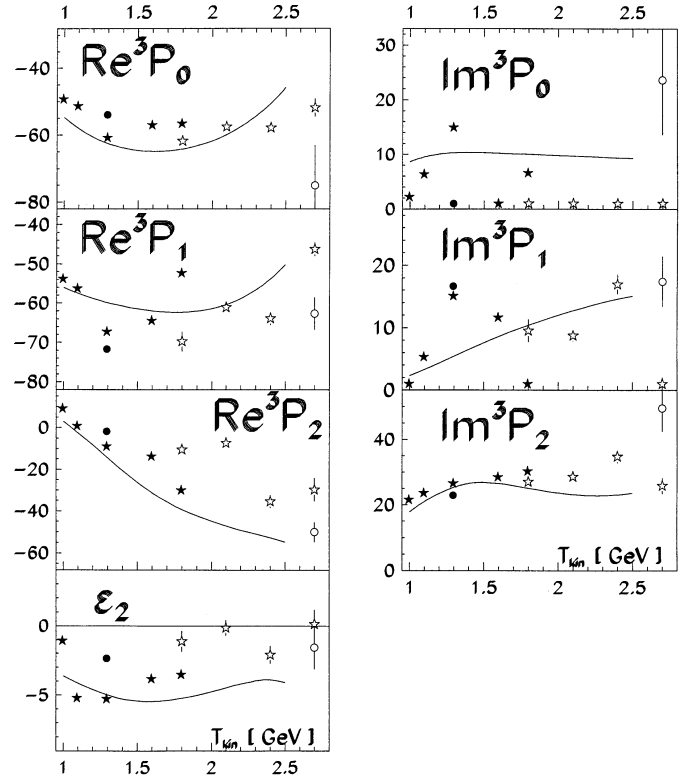


Fig. 2. Phase shift analyses results: Real and imaginary parts of 3P_0 , 3P_1 , 3P_2 , and mixing parameter ϵ_2 . Symbols are as in Fig. 1

In the forward direction, amplitude $e = 0$ and $a(0) - b(0) = c(0) + d(0)$. Three “optical theorems” linearly relate the imaginary parts of the non-vanishing amplitudes with three total cross sections. The general expression of the total cross section for a polarized nucleon beam transmitted through a polarized proton target, with arbitrary directions of beam and target polarizations, was first deduced in [50, 51]. Following [49] it is written in the form

$$\sigma_{tot} = \sigma_{0tot} + \sigma_{1tot}(\mathbf{P}_B, \mathbf{P}_T) + \sigma_{2tot}(\mathbf{P}_B, \mathbf{k})(\mathbf{P}_T, \mathbf{k}) \quad (2.3)$$

where \mathbf{P}_B and \mathbf{P}_T are the beam and target polarization. The term σ_{0tot} is the spin-independent total cross section, σ_{1tot} and σ_{2tot} are the spin-dependent contributions. They are related to the forward scattering amplitudes

$$\sigma_{0tot} = (2\pi/K)\Im m [a(0) + b(0)] \quad (2.4a)$$

$$\sigma_{1tot} = (2\pi/K)\Im m [c(0) + d(0)] \quad (2.4b)$$

$$\sigma_{2tot} = -(4\pi/K)\Im m [d(0)] \quad (2.4c)$$

where K is the wave number in the CM system.

The total cross sections σ_{tot} and σ_{0tot} are positive definite quantities. The spin-dependent contributions σ_{1tot} and σ_{2tot} are related to measurable quantities $\Delta\sigma_T$ and $\Delta\sigma_L$ by

$$-\Delta\sigma_T = 2\sigma_{1tot} \quad (2.5)$$

$$-\Delta\sigma_L = 2(\sigma_{1tot} + \sigma_{2tot}). \quad (2.6)$$

Table 3. Scattering amplitudes at 1.80 GeV. The ratios of χ^2/DF are given in brackets after the solution number in all following tables

Amplitude ($\sqrt{\text{mb/sr}}$)	$\theta = 32.6^\circ$ Sol. 1 (0.47)	$\theta = 32.6^\circ$ Sol. 2 (0.42)	$\theta = 35.9^\circ$ Sol. 1 (0.63)	$\theta = 35.9^\circ$ Sol. 2 (0.50)
$\Re a$	$+0.817 \pm 0.184$	$+1.838 \pm 0.437$	$+0.732 \pm 0.114$	$+1.298 \pm 0.506$
$\Im m a$	$+1.243 \pm 0.421$	$+1.449 \pm 0.474$	$+1.256 \pm 0.235$	-1.560 ± 0.239
$\Re b$	$+0.478 \pm 0.313$	$+0.725 \pm 0.903$	$+0.344 \pm 0.284$	$+0.881 \pm 0.478$
$\Im m b$	$+1.904 \pm 0.148$	$+1.626 \pm 0.554$	$+1.604 \pm 0.096$	-1.344 ± 0.370
$\Re c$	-0.360 ± 0.350	-0.028 ± 0.405	-0.346 ± 0.236	-0.497 ± 0.209
$\Im m c$	-0.171 ± 0.483	-0.915 ± 0.174	-0.192 ± 0.349	-0.113 ± 0.236
$\Re d$	-0.790 ± 0.388	-0.227 ± 0.171	-0.705 ± 0.144	-0.561 ± 0.156
$\Im m d$	-0.125 ± 0.316	-0.858 ± 0.174	-0.123 ± 0.247	-0.101 ± 0.171
$\Re e$	$+2.059 \pm 0.459$	$+0.915 \pm 0.219$	$+1.631 \pm 0.245$	$+0.919 \pm 0.358$
Amplitude ($\sqrt{\text{mb/sr}}$)	$\theta = 35.9^\circ$ Sol. 3 (0.59)	$\theta = 37.9^\circ$ Sol. 1 (0.95)	$\theta = 37.9^\circ$ Sol. 2 (0.84)	$\theta = 40.9^\circ$ Sol. 1 (0.40)
$\Re a$	$+1.828 \pm 0.511$	$+0.814 \pm 0.183$	$+1.577 \pm 0.665$	$+1.059 \pm 0.395$
$\Im m a$	$+1.072 \pm 0.781$	$+1.401 \pm 0.152$	-1.167 ± 0.759	$+1.251 \pm 0.231$
$\Re b$	$+1.591 \pm 0.137$	$+0.291 \pm 0.373$	$+0.843 \pm 0.617$	$+1.185 \pm 0.193$
$\Im m b$	-0.296 ± 0.738	$+1.466 \pm 0.112$	-1.244 ± 0.438	$+0.463 \pm 0.443$
$\Re c$	-0.386 ± 0.252	-0.460 ± 0.194	-0.412 ± 0.209	-0.277 ± 0.181
$\Im m c$	$+0.298 \pm 0.295$	-0.103 ± 0.426	-0.130 ± 0.255	-0.097 ± 0.262
$\Re d$	-0.144 ± 0.220	-0.417 ± 0.179	-0.312 ± 0.178	-0.051 ± 0.138
$\Im m d$	-0.583 ± 0.156	-0.113 ± 0.369	-0.015 ± 0.191	-0.367 ± 0.136
$\Re e$	$+0.652 \pm 0.182$	$+1.237 \pm 0.274$	$+0.638 \pm 0.269$	$+0.616 \pm 0.227$
Amplitude ($\sqrt{\text{mb/sr}}$)	$\theta = 40.9^\circ$ Sol. 2 (0.59)	$\theta = 45.8^\circ$ Sol. 1 (0.32)	$\theta = 45.8^\circ$ Sol. 2 (0.31)	$\theta = 51.2^\circ$ Sol. 1 (0.41)
$\Re a$	$+1.059 \pm 0.395$	$+0.356 \pm 0.050$	$+0.459 \pm 0.114$	$+0.199 \pm 0.032$
$\Im m a$	$+1.251 \pm 0.231$	$+0.887 \pm 0.107$	$+1.046 \pm 0.069$	$+0.565 \pm 0.103$
$\Re b$	$+1.185 \pm 0.193$	$+0.128 \pm 0.204$	$+0.074 \pm 0.291$	$+0.310 \pm 0.220$
$\Im m b$	$+0.463 \pm 0.443$	$+0.954 \pm 0.057$	$+0.933 \pm 0.062$	$+0.647 \pm 0.119$
$\Re c$	-0.277 ± 0.181	-0.023 ± 0.251	$+0.077 \pm 0.246$	$+0.052 \pm 0.175$
$\Im m c$	-0.097 ± 0.262	-0.287 ± 0.154	-0.354 ± 0.067	-0.201 ± 0.071
$\Re d$	-0.051 ± 0.138	-0.359 ± 0.156	$+0.032 \pm 0.127$	-0.255 ± 0.089
$\Im m d$	-0.367 ± 0.136	-0.225 ± 0.110	-0.352 ± 0.054	-0.160 ± 0.086
$\Re e$	$+0.616 \pm 0.227$	$+0.915 \pm 0.113$	$+0.708 \pm 0.170$	$+0.739 \pm 0.094$
Amplitude ($\sqrt{\text{mb/sr}}$)	$\theta = 51.2^\circ$ Sol. 2 (0.45)	$\theta = 55.5^\circ$ Sol. 1 (0.37)	$\theta = 55.5^\circ$ Sol. 2 (0.32)	$\theta = 66.0^\circ$ Sol. 1 (0.64)
$\Re a$	$+0.227 \pm 0.056$	$+0.150 \pm 0.031$	$+0.165 \pm 0.048$	$+0.037 \pm 0.005$
$\Im m a$	$+0.673 \pm 0.126$	$+0.497 \pm 0.113$	$+0.559 \pm 0.144$	$+0.282 \pm 0.037$
$\Re b$	$+0.086 \pm 0.215$	$+0.414 \pm 0.171$	$+0.473 \pm 0.110$	$+0.205 \pm 0.134$
$\Im m b$	$+0.689 \pm 0.072$	$+0.448 \pm 0.162$	$+0.382 \pm 0.124$	$+0.408 \pm 0.071$
$\Re c$	$+0.175 \pm 0.215$	-0.267 ± 0.086	$+0.268 \pm 0.089$	$+0.095 \pm 0.101$
$\Im m c$	-0.216 ± 0.080	$+0.055 \pm 0.165$	-0.069 ± 0.115	-0.188 ± 0.035
$\Re d$	$+0.070 \pm 0.183$	$+0.124 \pm 0.123$	-0.238 ± 0.092	-0.070 ± 0.139
$\Im m d$	-0.228 ± 0.094	-0.204 ± 0.072	$+0.067 \pm 0.076$	-0.178 ± 0.073
$\Re e$	$+0.657 \pm 0.145$	$+0.656 \pm 0.104$	$+0.596 \pm 0.150$	$+0.594 \pm 0.026$
Amplitude ($\sqrt{\text{mb/sr}}$)	$\theta = 73.9^\circ$ Sol. 1 (0.42)	$\theta = 73.9^\circ$ Sol. 2 (0.45)	$\theta = 81.9^\circ$ Sol. 1 (0.62)	$\theta = 81.9^\circ$ Sol. 2 (0.40)
$\Re a$	$+0.032 \pm 0.004$	$+0.033 \pm 0.005$	$+0.012 \pm 0.004$	$+0.011 \pm 0.004$
$\Im m a$	$+0.121 \pm 0.054$	$+0.188 \pm 0.030$	$+0.085 \pm 0.055$	$+0.107 \pm 0.038$
$\Re b$	$+0.166 \pm 0.110$	-0.015 ± 0.157	$+0.144 \pm 0.103$	-0.052 ± 0.129
$\Im m b$	$+0.314 \pm 0.062$	$+0.364 \pm 0.020$	$+0.260 \pm 0.063$	$+0.297 \pm 0.035$
$\Re c$	-0.136 ± 0.068	-0.054 ± 0.088	$+0.157 \pm 0.058$	-0.127 ± 0.065
$\Im m c$	-0.145 ± 0.042	-0.174 ± 0.031	-0.158 ± 0.041	-0.177 ± 0.035
$\Re d$	-0.190 ± 0.052	$+0.139 \pm 0.067$	-0.204 ± 0.046	$+0.171 \pm 0.059$
$\Im m d$	-0.109 ± 0.061	-0.180 ± 0.028	-0.092 ± 0.059	-0.141 ± 0.045
$\Re e$	$+0.587 \pm 0.022$	$+0.566 \pm 0.024$	$+0.579 \pm 0.022$	$+0.576 \pm 0.022$

Table 3. (continued)

Amplitudes at 1.80 GeV. The ratios of χ^2/DF are given in brackets after the solution number			
Amplitude ($\sqrt{mb/sr}$)	$\theta = 86.5^\circ$ Sol. 1 (0.66)	$\theta = 86.5^\circ$ Sol. 2 (0.68)	$\theta = 90.0^\circ$ Sol. 1 (0.85)
$\Re a$	$+0.001 \pm 0.004$	$+0.001 \pm 0.004$	-0.013 ± 0.004
$\Im m a$	$+0.043 \pm 0.045$	$+0.034 \pm 0.039$	$+0.032 \pm 0.041$
$\Re b$	$+0.109 \pm 0.108$	-0.059 ± 0.114	$+0.108 \pm 0.112$
$\Im m b$	$+0.250 \pm 0.057$	$+0.264 \pm 0.042$	$+0.267 \pm 0.053$
$\Re c$	$+0.156 \pm 0.064$	-0.156 ± 0.064	$+0.077 \pm 0.090$
$\Im m c$	-0.180 ± 0.040	-0.183 ± 0.039	-0.182 ± 0.034
$\Re d$	-0.199 ± 0.054	$+0.183 \pm 0.058$	-0.185 ± 0.061
$\Im m d$	-0.114 ± 0.056	-0.132 ± 0.048	-0.140 ± 0.046
$\Re e$	$+0.603 \pm 0.022$	$+0.605 \pm 0.022$	$+0.606 \pm 0.018$

In the forward direction, the quantity

$$\rho = \Re [a(0) + b(0)] / \Im [a(0) + b(0)] \quad (2.7)$$

can be calculated using the dispersion relation calculations [37]. The integral of the differential cross section is the total elastic cross section $\sigma_{tot}(\text{el.})$. The difference $\sigma_{0tot} - \sigma_{tot}(\text{el.})$ is the total inelastic or reaction cross section $\sigma_{tot}(\text{inel.})$. It can also be determined as the sum of individual reaction total cross sections over all inelastic reaction channels [36]. The measured observables given in (2.4a), (2.5) and (2.6), the calculated quantities given in (2.7) and $\sigma_{tot}(\text{inel.})$ are introduced in the PSA, but are not used the DRSA because it is not performed in the forward direction.

In the following we give relations between scattering amplitudes and observables at any angle. Only the observables used in the analyses are listed. We denote by θ the CM scattering angle and by θ_2 the laboratory angle of the recoil particle.

$$\sigma = \frac{d\sigma}{d\Omega} = \frac{1}{2} [|a|^2 + |b|^2 + |c|^2 + |d|^2 + |e|^2] \quad (2.8)$$

$$\sigma A_{oonn} = \frac{1}{2} [|a|^2 - |b|^2 - |c|^2 + |d|^2 + |e|^2] \quad (2.9)$$

$$\sigma D_{onon} = \frac{1}{2} [|a|^2 + |b|^2 - |c|^2 - |d|^2 + |e|^2] \quad (2.10)$$

$$\sigma K_{onno} = \frac{1}{2} [|a|^2 - |b|^2 + |c|^2 - |d|^2 + |e|^2] \quad (2.11)$$

$$\sigma A_{oono} = \sigma A_{oonn} = \sigma P_{onoo} = \sigma N_{onnn} = \Re a^* e \quad (2.12)$$

$$\sigma A_{ooss} = +\Re a^* d \cos \theta - \Im m d^* e \sin \theta + \Re b^* c \quad (2.13)$$

$$\sigma A_{ookk} = -\Re a^* d \cos \theta + \Im m d^* e \sin \theta + \Re b^* c \quad (2.14)$$

$$\sigma A_{oosk} = -\Re a^* d \sin \theta - \Im m d^* e \cos \theta \quad (2.15)$$

$$\sigma D_{os'ok} = +\Re a^* b \sin(\theta + \theta_2) - \Re c^* d \sin \theta_2 + \Im m b^* e \cos(\theta + \theta_2) \quad (2.16)$$

$$\sigma K_{os'os} = -\Re a^* c \cos(\theta + \theta_2) - \Re b^* d \cos \theta_2 + \Im m c^* e \sin(\theta + \theta_2) \quad (2.17)$$

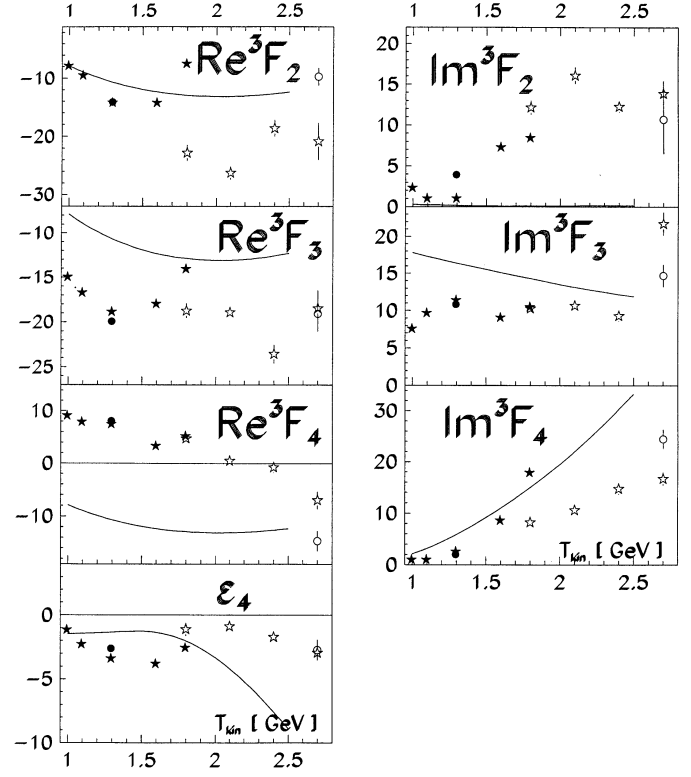


Fig. 3. Phase shift analyses results: Real and imaginary parts of 3F_2 , 3F_3 , 3F_4 , and mixing parameter ϵ_4 . Symbols are as in Fig. 1

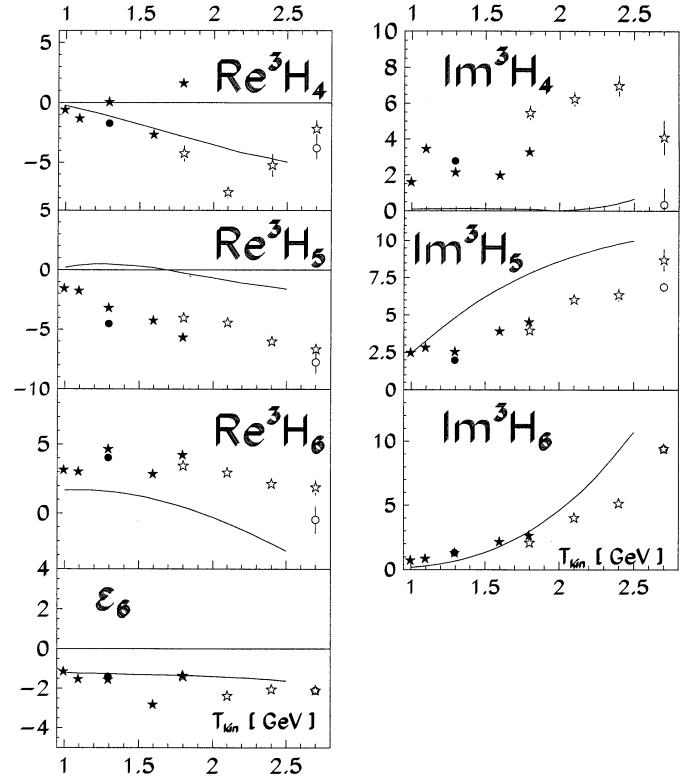


Fig. 4. Phase shift analyses results: Real and imaginary parts of 3H_4 , 3H_5 , 3H_6 , and mixing parameter ϵ_6 . Symbols are as in Fig. 1

Table 4. Scattering amplitudes at 2.10 GeV. The ratios of χ^2/DF are given in brackets after the solution number

Amplitude ($\sqrt{mb/sr}$)	$\theta = 33.0^\circ$ Sol. 1 (0.59)	$\theta = 33.0^\circ$ Sol. 2 (0.46)	$\theta = 36.0^\circ$ Sol. 3 (0.59)	$\theta = 36.0^\circ$ Sol. 1 (0.47)
$\Re a$	$+0.638 \pm 0.090$	$+0.677 \pm 0.289$	$+1.322 \pm 0.492$	$+0.535 \pm 0.129$
$\Im a$	$+1.063 \pm 0.252$	-1.267 ± 0.647	$+1.352 \pm 0.281$	$+1.064 \pm 0.274$
$\Re b$	$+0.001 \pm 0.260$	$+0.198 \pm 0.241$	$+0.415 \pm 0.653$	-0.063 ± 0.285
$\Im b$	$+1.574 \pm 0.091$	-1.632 ± 0.053	-1.505 ± 0.171	$+1.320 \pm 0.065$
$\Re c$	-0.044 ± 0.225	$+0.303 \pm 0.206$	$+0.464 \pm 0.234$	$+0.083 \pm 0.250$
$\Im c$	-0.568 ± 0.258	-0.041 ± 0.124	-0.377 ± 0.255	-0.357 ± 0.206
$\Re d$	-0.157 ± 0.234	-0.027 ± 0.119	$+0.565 \pm 0.221$	-0.099 ± 0.296
$\Im d$	-0.506 ± 0.201	-0.219 ± 0.094	$+0.240 \pm 0.179$	-0.315 ± 0.181
$\Re e$	$+1.643 \pm 0.222$	$+1.552 \pm 0.660$	$+0.794 \pm 0.296$	$+1.283 \pm 0.302$
Amplitude ($\sqrt{mb/sr}$)	$\theta = 36.0^\circ$ Sol. 2 (0.36)	$\theta = 38.0^\circ$ Sol. 1 (0.54)	$\theta = 38.0^\circ$ Sol. 2 (0.54)	$\theta = 41.0^\circ$ Sol. 1 (0.48)
$\Re a$	$+0.781 \pm 0.257$	$+0.525 \pm 0.187$	$+0.722 \pm 0.367$	$+0.389 \pm 0.077$
$\Im a$	-1.314 ± 0.053	$+1.106 \pm 0.192$	$+1.192 \pm 0.050$	$+0.870 \pm 0.111$
$\Re b$	$+0.170 \pm 0.193$	$+0.077 \pm 0.316$	-0.135 ± 0.241	$+0.321 \pm 0.182$
$\Im b$	-1.316 ± 0.066	$+1.221 \pm 0.056$	$+1.204 \pm 0.052$	$+0.930 \pm 0.079$
$\Re c$	$+0.342 \pm 0.205$	$+0.132 \pm 0.233$	-0.300 ± 0.157	$+0.225 \pm 0.183$
$\Im c$	-0.043 ± 0.110	-0.262 ± 0.145	$+0.170 \pm 0.263$	-0.201 ± 0.161
$\Re d$	-0.122 ± 0.142	$+0.097 \pm 0.208$	$+0.277 \pm 0.179$	$+0.216 \pm 0.167$
$\Im d$	-0.218 ± 0.112	-0.269 ± 0.140	$+0.030 \pm 0.209$	-0.283 ± 0.160
$\Re e$	$+0.880 \pm 0.285$	$+0.973 \pm 0.342$	$+0.710 \pm 0.362$	$+0.850 \pm 0.161$
Amplitude ($\sqrt{mb/sr}$)	$\theta = 41.0^\circ$ Sol. 2 (0.56)	$\theta = 45.8^\circ$ Sol. 1 (0.78)	$\theta = 45.8^\circ$ Sol. 2 (0.50)	$\theta = 55.1^\circ$ Sol. 1 (1.00)
$\Re a$	$+0.741 \pm 0.279$	$+0.233 \pm 0.037$	$+0.532 \pm 0.285$	$+0.081 \pm 0.021$
$\Im a$	-0.952 ± 0.157	$+0.650 \pm 0.090$	-0.752 ± 0.142	$+0.325 \pm 0.069$
$\Re b$	$+0.597 \pm 0.193$	$+0.223 \pm 0.132$	$+0.568 \pm 0.242$	$+0.195 \pm 0.105$
$\Im b$	-0.770 ± 0.163	$+0.672 \pm 0.052$	-0.394 ± 0.362	$+0.462 \pm 0.051$
$\Re c$	-0.096 ± 0.155	$+0.192 \pm 0.096$	$+0.341 \pm 0.061$	$+0.197 \pm 0.073$
$\Im c$	-0.322 ± 0.107	-0.279 ± 0.063	$+0.140 \pm 0.159$	-0.145 ± 0.061
$\Re d$	$+0.115 \pm 0.107$	-0.056 ± 0.174	$+0.073 \pm 0.124$	-0.122 ± 0.101
$\Im d$	-0.194 ± 0.087	-0.182 ± 0.070	-0.249 ± 0.065	-0.114 ± 0.066
$\Re e$	$+0.466 \pm 0.166$	$+0.704 \pm 0.099$	$+0.308 \pm 0.165$	$+0.589 \pm 0.049$

$$\sigma K_{os''ko} = +\Re a^* c \sin(\theta + \theta_2) - \Re b^* d \sin \theta_2 + \Im c^* e \cos(\theta + \theta_2) \quad (2.18)$$

$$\sigma K_{ok''so} = -\Re a^* c \sin(\theta + \theta_2) - \Re b^* d \sin \theta_2 - \Im c^* e \cos(\theta + \theta_2) \quad (2.19)$$

$$\sigma K_{ok''ko} = -\Re a^* c \cos(\theta + \theta_2) + \Re b^* d \cos \theta_2 + \Im c^* e \sin(\theta + \theta_2) \quad (2.20)$$

$$\sigma N_{onsk} = -\Re d^* e \sin \theta + \Im a^* d \cos \theta + \Im b^* c \quad (2.21)$$

$$\sigma N_{onkk} = +\Re d^* e \cos \theta + \Im a^* d \sin \theta \quad (2.22)$$

$$\sigma N_{os''sn} = -\Re c^* e \cos(\theta + \theta_2) - \Im b^* d \sin \theta_2 - \Im a^* c \sin(\theta + \theta_2) \quad (2.23)$$

$$\sigma N_{os''nk} = +\Re b^* e \sin(\theta + \theta_2) + \Im c^* d \cos \theta_2 - \Im a^* b \cos(\theta + \theta_2) \quad (2.24)$$

$$\sigma N_{ok''nk} = -\Re b^* e \cos(\theta + \theta_2) + \Im c^* d \sin \theta_2 - \Im a^* b \sin(\theta + \theta_2) \quad (2.25)$$

$$\sigma N_{os''kn} = +\Re c^* e \sin(\theta + \theta_2) + \Im b^* d \cos \theta_2 - \Im a^* c \cos(\theta + \theta_2) \quad (2.26)$$

$$\sigma N_{ok''kn} = -\Re c^* e \cos(\theta + \theta_2) + \Im b^* d \sin \theta_2 - \Im a^* c \sin(\theta + \theta_2) \quad (2.27)$$

The differential cross section is the only absolute quantity (mb/sr). The spin-dependent observables, multiplied by the differential cross section, are bilinear combinations of the real and imaginary parts of amplitudes. The bilinear terms are invariant with respect to the introduction of an arbitrary phase common to all amplitudes. In the DRSA we forced the amplitude e to be real, i.e

$$e = \Re e = |e| \geq 0, \quad \Im e = 0, \quad \phi_e = 0. \quad (2.28)$$

All amplitude phases are then given relative to ϕ_e , and only 9 parameters are to be determined in the DRSA.

In the PSA the scattering amplitudes are developed into series of Legendre polynomials and the partial wave

Table 4. (continued)

Results at 2.10 GeV. The ratios of χ^2/DF are given in brackets after the solution number

Amplitude ($\sqrt{mb/sr}$)	$\theta = 55.1^\circ$ Sol. 2 (0.82)	$\theta = 55.1^\circ$ Sol. 3 (0.75)	$\theta = 65.0^\circ$ Sol. 1 (1.19)	$\theta = 73.7^\circ$ Sol. 1 (0.86)
Re a	+0.130 \pm 0.063	+0.172 \pm 0.080	+0.061 \pm 0.005	+0.055 \pm 0.004
Im a	+0.555 \pm 0.089	-0.598 \pm 0.046	+0.170 \pm 0.046	+0.080 \pm 0.043
Re b	+0.303 \pm 0.129	+0.324 \pm 0.126	+0.224 \pm 0.072	+0.202 \pm 0.078
Im b	+0.382 \pm 0.091	-0.383 \pm 0.115	+0.326 \pm 0.051	+0.274 \pm 0.058
Re c	+0.282 \pm 0.053	+0.257 \pm 0.043	+0.100 \pm 0.051	+0.017 \pm 0.072
Im c	+0.041 \pm 0.065	+0.072 \pm 0.081	-0.183 \pm 0.029	-0.166 \pm 0.023
Re d	+0.113 \pm 0.078	-0.097 \pm 0.053	-0.125 \pm 0.052	-0.161 \pm 0.041
Im d	+0.067 \pm 0.060	-0.080 \pm 0.044	-0.128 \pm 0.050	-0.126 \pm 0.047
Re e	+0.369 \pm 0.152	+0.268 \pm 0.112	+0.517 \pm 0.026	+0.492 \pm 0.022
Amplitude ($\sqrt{mb/sr}$)	$\theta = 73.7^\circ$ Sol. 2 (0.90)	$\theta = 73.7^\circ$ Sol. 3 (1.05)	$\theta = 82.0^\circ$ Sol. 1 (0.81)	$\theta = 82.0^\circ$ Sol. 2 (0.85)
Re a	+0.060 \pm 0.006	+0.067 \pm 0.010	+0.030 \pm 0.004	+0.031 \pm 0.004
Im a	+0.195 \pm 0.041	+0.294 \pm 0.067	+0.016 \pm 0.033	+0.088 \pm 0.042
Re b	-0.198 \pm 0.079	+0.341 \pm 0.018	+0.117 \pm 0.060	-0.146 \pm 0.070
Im b	+0.274 \pm 0.054	+0.033 \pm 0.040	+0.232 \pm 0.034	+0.207 \pm 0.050
Re c	+0.025 \pm 0.074	+0.107 \pm 0.030	-0.026 \pm 0.061	-0.011 \pm 0.064
Im c	-0.169 \pm 0.023	-0.124 \pm 0.030	-0.183 \pm 0.021	-0.193 \pm 0.018
Re d	+0.138 \pm 0.051	-0.197 \pm 0.021	-0.150 \pm 0.027	+0.155 \pm 0.036
Im d	-0.155 \pm 0.037	+0.033 \pm 0.023	-0.114 \pm 0.019	-0.101 \pm 0.038
Re e	+0.457 \pm 0.028	+0.403 \pm 0.053	+0.465 \pm 0.022	+0.459 \pm 0.023
Amplitude ($\sqrt{mb/sr}$)	$\theta = 85.4^\circ$ Sol. 1 (0.56)	$\theta = 85.4^\circ$ Sol. 2 (0.49)	$\theta = 90.0^\circ$ Sol. 1 (0.74)	$\theta = 90.0^\circ$ Sol. 2 (0.57)
Re a	+0.020 \pm 0.004	+0.020 \pm 0.004	-0.008 \pm 0.003	-0.008 \pm 0.004
Im a	+0.011 \pm 0.031	+0.036 \pm 0.036	+0.012 \pm 0.028	-0.028 \pm 0.043
Re b	+0.115 \pm 0.058	-0.090 \pm 0.069	+0.083 \pm 0.048	-0.131 \pm 0.050
Im b	+0.221 \pm 0.033	+0.222 \pm 0.034	+0.184 \pm 0.025	-0.151 \pm 0.048
Re c	-0.050 \pm 0.057	-0.057 \pm 0.053	-0.068 \pm 0.051	-0.088 \pm 0.047
Im c	-0.186 \pm 0.024	-0.195 \pm 0.021	-0.205 \pm 0.021	-0.216 \pm 0.020
Re d	-0.143 \pm 0.027	+0.154 \pm 0.032	-0.124 \pm 0.025	+0.160 \pm 0.026
Im d	-0.118 \pm 0.015	-0.101 \pm 0.030	-0.114 \pm 0.009	-0.062 \pm 0.040
Re e	+0.481 \pm 0.022	+0.480 \pm 0.022	+0.439 \pm 0.011	+0.459 \pm 0.012

amplitudes $S_J, S_{JJ}, S_{J-1,J}, S_{J+1,J}, S^J$ are independent of the scattering angle [52–55]. The partial wave amplitudes depend on phase shifts δ_{LJ} , labeled with orbital and total angular momentum subscripts. According to the spectroscopic notation, the orbital angular momenta L ranging from 0 to 10 are denoted by capital letters S, P, D, F, G, H, I, J, L, M, N, respectively. The subscripts denote the total angular momentum and the superscripts denote the spin state (singlet or triplet). For the nucleon-nucleon interaction one has

$$(-1)^{L+s+I} = -1 \quad (2.29)$$

where I is the isospin. The spectroscopic notation is used in the tables and figures below.

For singlet and uncoupled-triplet partial waves ($L = J$), we have

$$S_J = \exp(2i\delta_J), \quad S_{JJ} = \exp(2i\delta_{JJ}). \quad (2.30)$$

Coupled-triplet partial wave amplitudes also contain mixing parameters ϵ_J which relate phase shifts with the orbital momenta $L = J \pm 1$.

$$S_{J-1,J} = \cos 2\epsilon_J \exp[2i\delta_{J-1,J}] - 1, \quad (2.31)$$

$$S^J = i \sin 2\epsilon_J \exp[i(\delta_{J+1,J} + \delta_{J-1,J})]. \quad (2.32)$$

The infinite polynomial series are cut at the orbital angular momentum L_{max} . Residual terms from L_{max} to infinity are replaced by the peripheral part of the interaction, well described by the one-pion-exchange contribution (OPE) [53–55]. The introduction of OPE contribution also insures stability of the PSA solutions, i.e. the low phase shifts change very little if L_{max} is changed. The OPE contribution, calculated from the Born approximation, supplements only the real parts of higher phase shifts.

The aim of phase shift analyses is to determine the nuclear part of the interaction, namely “nuclear bar phase shifts”. The known electromagnetic amplitudes depending

Table 5. Scattering amplitudes at 2.40 GeV. The ratios of χ^2/DF are given in brackets after the solution number

Amplitude ($\sqrt{mb/sr}$)	$\theta = 29.3^\circ$ Sol. 1 (0.89)	$\theta = 29.3^\circ$ Sol. 2 (0.88)	$\theta = 38.8^\circ$ Sol. 1 (0.51)	$\theta = 38.8^\circ$ Sol. 2 (0.31)
$\Re a$	$+1.599 \pm 0.680$	$+1.767 \pm 0.578$	$+0.355 \pm 0.078$	$+0.491 \pm 0.207$
$\Im m a$	$+1.581 \pm 0.508$	$+1.461 \pm 0.553$	$+0.859 \pm 0.129$	$+0.932 \pm 0.074$
$\Re b$	$+1.721 \pm 0.474$	$+2.066 \pm 0.110$	$+0.440 \pm 0.301$	$+0.697 \pm 0.254$
$\Im m b$	$+0.957 \pm 0.798$	$+0.220 \pm 0.730$	$+0.831 \pm 0.162$	$+0.598 \pm 0.278$
$\Re c$	$+0.296 \pm 0.413$	-0.032 ± 0.549	$+0.263 \pm 0.270$	-0.362 ± 0.172
$\Im m c$	-0.610 ± 0.311	-0.158 ± 0.519	-0.194 ± 0.263	$+0.129 \pm 0.210$
$\Re d$	$+0.459 \pm 0.314$	$+0.356 \pm 0.319$	-0.202 ± 0.282	$+0.230 \pm 0.166$
$\Im m d$	-0.515 ± 0.390	-0.519 ± 0.386	$+0.022 \pm 0.234$	-0.228 ± 0.142
$\Re e$	$+0.842 \pm 0.354$	$+0.766 \pm 0.248$	$+0.809 \pm 0.168$	$+0.586 \pm 0.242$
Amplitude ($\sqrt{mb/sr}$)	$\theta = 38.8^\circ$ Sol. 3 (0.36)	$\theta = 51.3^\circ$ Sol. 1 (0.96)	$\theta = 51.3^\circ$ Sol. 2 (1.03)	$\theta = 51.3^\circ$ Sol. 3 (1.19)
$\Re a$	$+0.722 \pm 0.575$	$+0.116 \pm 0.040$	$+0.149 \pm 0.084$	$+0.184 \pm 0.079$
$\Im m a$	-0.916 ± 0.326	$+0.387 \pm 0.140$	$+0.477 \pm 0.118$	-0.526 ± 0.036
$\Re b$	$+0.783 \pm 0.513$	$+0.313 \pm 0.212$	$+0.341 \pm 0.267$	$+0.269 \pm 0.155$
$\Im m b$	-0.542 ± 0.772	$+0.361 \pm 0.182$	$+0.372 \pm 0.229$	-0.439 ± 0.103
$\Re c$	$+0.112 \pm 0.257$	$+0.226 \pm 0.209$	-0.168 ± 0.099	$+0.142 \pm 0.082$
$\Im m c$	$+0.265 \pm 0.209$	$+0.069 \pm 0.198$	$+0.058 \pm 0.084$	$+0.006 \pm 0.109$
$\Re d$	-0.172 ± 0.135	-0.198 ± 0.090	-0.147 ± 0.187	$+0.007 \pm 0.079$
$\Im m d$	-0.117 ± 0.144	$+0.110 \pm 0.066$	-0.124 ± 0.114	$+0.114 \pm 0.067$
$\Re e$	$+0.398 \pm 0.317$	$+0.426 \pm 0.135$	$+0.328 \pm 0.177$	$+0.268 \pm 0.108$
Amplitude ($\sqrt{mb/sr}$)	$\theta = 51.3^\circ$ Sol. 4 (0.71)	$\theta = 65.6^\circ$ Sol. 1 (0.90)	$\theta = 65.6^\circ$ Sol. 2 (0.90)	$\theta = 65.6^\circ$ Sol. 3 (0.90)
$\Re a$	$+0.237 \pm 0.309$	$+0.094 \pm 0.030$	$+0.197 \pm 0.157$	$+0.236 \pm 0.310$
$\Im m a$	-0.532 ± 0.047	$+0.264 \pm 0.142$	-0.310 ± 0.033	-0.358 ± 0.135
$\Re b$	$+0.378 \pm 0.334$	$+0.232 \pm 0.140$	$+0.099 \pm 0.182$	$+0.289 \pm 0.164$
$\Im m b$	-0.293 ± 0.422	$+0.231 \pm 0.137$	-0.312 ± 0.066	-0.154 ± 0.306
$\Re c$	-0.085 ± 0.227	-0.120 ± 0.064	$+0.134 \pm 0.056$	-0.063 ± 0.108
$\Im m c$	-0.225 ± 0.091	$+0.069 \pm 0.095$	-0.035 ± 0.094	-0.123 ± 0.066
$\Re d$	$+0.040 \pm 0.082$	-0.142 ± 0.059	$+0.118 \pm 0.049$	-0.145 ± 0.043
$\Im m d$	$+0.101 \pm 0.069$	-0.048 ± 0.113	$+0.093 \pm 0.053$	-0.038 ± 0.123
$\Re e$	$+0.205 \pm 0.267$	$+0.355 \pm 0.112$	$+0.170 \pm 0.136$	$+0.142 \pm 0.186$
Amplitude ($\sqrt{mb/sr}$)	$\theta = 82.6^\circ$ Sol. 1 (0.25)	$\theta = 82.6^\circ$ Sol. 2 (0.25)	$\theta = 82.6^\circ$ Sol. 3 (0.32)	$\theta = 82.6^\circ$ Sol. 4 (0.32)
$\Re a$	$+0.030 \pm 0.007$	$+0.032 \pm 0.012$	$+0.030 \pm 0.007$	$+0.030 \pm 0.007$
$\Im m a$	$+0.148 \pm 0.114$	$+0.184 \pm 0.150$	$+0.160 \pm 0.102$	$+0.157 \pm 0.101$
$\Re b$	-0.111 ± 0.131	$+0.041 \pm 0.141$	-0.075 ± 0.158	$+0.156 \pm 0.090$
$\Im m b$	$+0.172 \pm 0.085$	$+0.200 \pm 0.036$	$+0.191 \pm 0.063$	$+0.131 \pm 0.103$
$\Re c$	-0.136 ± 0.030	$+0.135 \pm 0.031$	-0.106 ± 0.085	$+0.137 \pm 0.028$
$\Im m c$	$+0.018 \pm 0.129$	$+0.025 \pm 0.091$	$+0.087 \pm 0.095$	$+0.015 \pm 0.125$
$\Re d$	$+0.101 \pm 0.045$	$+0.111 \pm 0.039$	-0.076 ± 0.061	-0.080 ± 0.049
$\Im m d$	$+0.059 \pm 0.053$	$+0.037 \pm 0.077$	$+0.082 \pm 0.048$	$+0.079 \pm 0.036$
$\Re e$	$+0.299 \pm 0.061$	$+0.278 \pm 0.102$	$+0.295 \pm 0.061$	$+0.296 \pm 0.060$

on the interacting particles and the interference terms are added to the nuclear part [56–59].

Below the one-pion-production threshold T_{Thr} the phase shifts δ and the mixing parameters ϵ_J are real and the unitarity condition automatically holds for the present S -matrix parametrization. The inelasticities present above T_{Thr} give rise to imaginary parts of the phase shifts [1].

Instead of the imaginary part of the mixing parameter ϵ_J the so-called “sixth parameter” α_J is introduced as follows [3, 60–62]:

$$S^J = i \sin 2\epsilon_J \exp [i(\delta_{J+1,J} + \delta_{J-1,J} + \alpha_J)] . \quad (2.33)$$

The calculations showed that this parameter does not affect the PSA results on the level of existing data accuracy.

3 PSA and amplitude analysis complementarity

In the following, we discuss the complementarity of the DRSA amplitude analysis and the PSA method, their relative advantages and limits. We stress the necessity of a check of PSA results by a direct reconstruction of the scattering matrix, whenever an amplitude analysis is possible.

The DRSA is performed at one energy and one angle, where it requires a complete set of measured observables [63]. For this reason it is always limited to a small number of angles and it will never be a universal tool predicting unknown quantities. The information provided by an accurately measured angular dependence of observables is lost, or may be used only indirectly to eliminate extraneous solutions. On the other hand, the amplitude analysis is completely model independent. It gives a pure phenomenological description of a given interaction channel without any additional conditions and has no energy limit. Since the solution at one angle is independent of those at other angles, the amplitude analysis can reveal possible anomalies in angular or energy dependences.

In the PSA approach the reconstruction of scattering amplitudes is possible even from incomplete sets of experimental quantities [64]. The lack of observables at some angles is compensated by imposed smooth functions of angle which average possible anomalies in the angular dependences of observables.

The differential cross section provides not only an absolute normalization at all angles, but, in addition, plays the same role as any other observable. Due to the angular continuity ensured by the parametrization, including the forward direction, and because the higher partial amplitudes are fixed by OPE, the common phase of scattering amplitudes is defined at all angles.

In an energy-dependent PSA, the phase shifts are parametrized as functions of energy, as explained in [2, 60]. This imposes a relatively smooth energy dependence on all parameters.

Assuming that the electromagnetic part of the nucleon-nucleon elastic scattering is well known, the PSA below the pion production threshold for a fixed isospin state is practically model independent. At these energies only OPE contribution may be considered as a weakly model-dependent part.

With increasing energy the peripheral interaction described by OPE is introduced at progressively higher L_{max} values. Due to the increasing importance of inelastic interactions phase shifts may become complex. This increases the number of free parameters. The only observable usable in the PSA which is directly related to the imaginary parts of phase shifts is the total inelastic cross section. The imaginary parts are poorly constrained for large angular momenta and must be taken from models. With increasing energy the PSA become more model dependent. An upper energy limit for the validity of the PSA method is however hard to estimate.

The best way of checking the validity of model-dependent contributions to a PSA is to compare the PSA amplitude predictions with the direct reconstruction from the

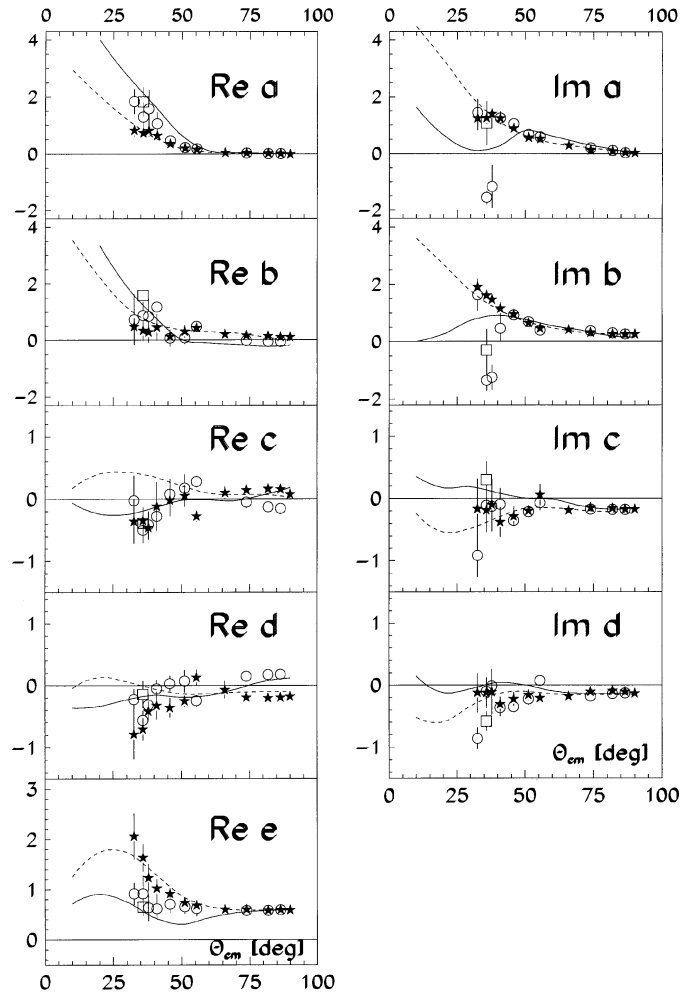


Fig. 5. Direct reconstruction of the scattering amplitudes at 1.80 GeV: the real and imaginary parts of amplitudes a to e are shown in $\sqrt{mb/sr}$ as a function of the CM angle. The dashed lines are the results of the present PSA, the solid line is the VPI PSA [66]

amplitude analysis. In this respect, the amplitude analysis is complementary to the PSA. Agreement supports the PSA which may then be used to predict unmeasured quantities. A disagreement between the two methods either suggests a possible anomaly in the database, or casts a doubt on the PSA theoretical input.

Comparison of PSA with directly-reconstructed amplitudes is also important at low energy close to the pion production threshold. The DRSA then provides a check of the validity of different potential models (not treated here, see [38]).

4 Database

The data used in the present PSA are summarized in Tables 1a and b. For each energy the number of data points for each observable are indicated as well as the χ^2 -values. The major part of the spin-dependent observables

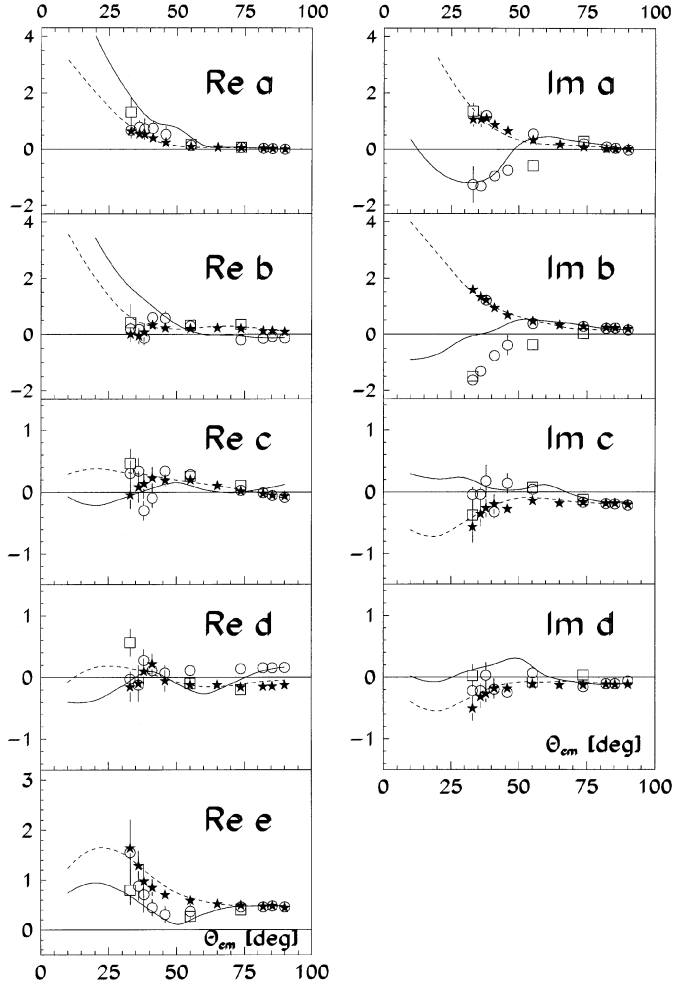


Fig. 6. Direct reconstruction of the scattering amplitudes at 2.10 GeV. See Fig. 5 for symbols

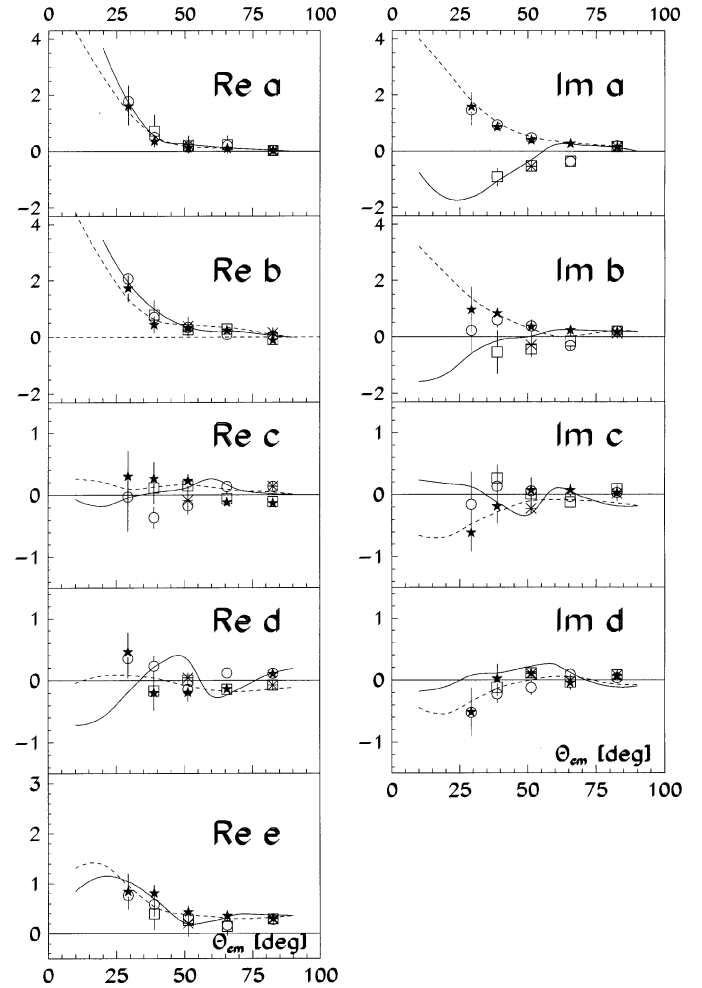


Fig. 7. Direct reconstruction of the scattering amplitudes at 2.40 GeV. See Fig. 5 for symbols

($\sim 94\%$) in the energy range were measured at SATURNE II [6–19].

The differential cross sections included in the analysis were often measured at energies which differed from the central values of the PSA or the DRSA. In those cases interpolation of the data was used.

Normalization factors for some data sets which gave excessively large contributions were introduced as free parameters in the PSA. The same normalization factors were employed in the DRSA data bases. Except for the 2.40 GeV A_{ono} data from ANL-ZGS [34] (normalization factor = 1.24) only differential cross sections data were normalized. The fact that these data were measured at slightly different energies from the central values of the PSA solutions might have affected the normalization factors. The recent precise COSY [32] results which have not been normalized play an important role.

In addition to the measured data, the values of ρ from [37] (with a 5% relative error) and the total inelastic cross sections from [36] were introduced into PSA.

5 Minimization procedure

At all energies, the search for PSA solutions was performed starting from random initial phase shift values[1]. The real part of the phase shifts starting from 3J_7 were fixed to the OPE contribution except for $\Re e {}^3J_8$ which was always fitted in accordance with our previous conclusions at 1.80 GeV [3]. The imaginary parts of the phase shifts starting from 3J_6 were fixed to the values of a dispersion relation calculation by the Paris group [48]. The imaginary parts at 1.80 and 2.10 GeV were fixed to zero starting at 3L_9 . At 2.40 and 2.70 GeV phases above $\Im m {}^3N_{10}$ were set to zero. It is obvious that different theoretical input for the high- L imaginary parts of phase shifts will change the PSA solutions.

At each of the three lower energies one solution was found. Due to a lack of data, $\Im m {}^3H_6$ and ϵ_6 were fixed by theoretical input at 2.70 GeV. Keeping these two phase shifts free provided a solution that was similar but the program had difficulty converging. At 2.70 GeV two different solutions were found. One was the solution obtained by starting the minimization procedure from the phase shifts at 2.40 GeV, the second one was obtained in a search with

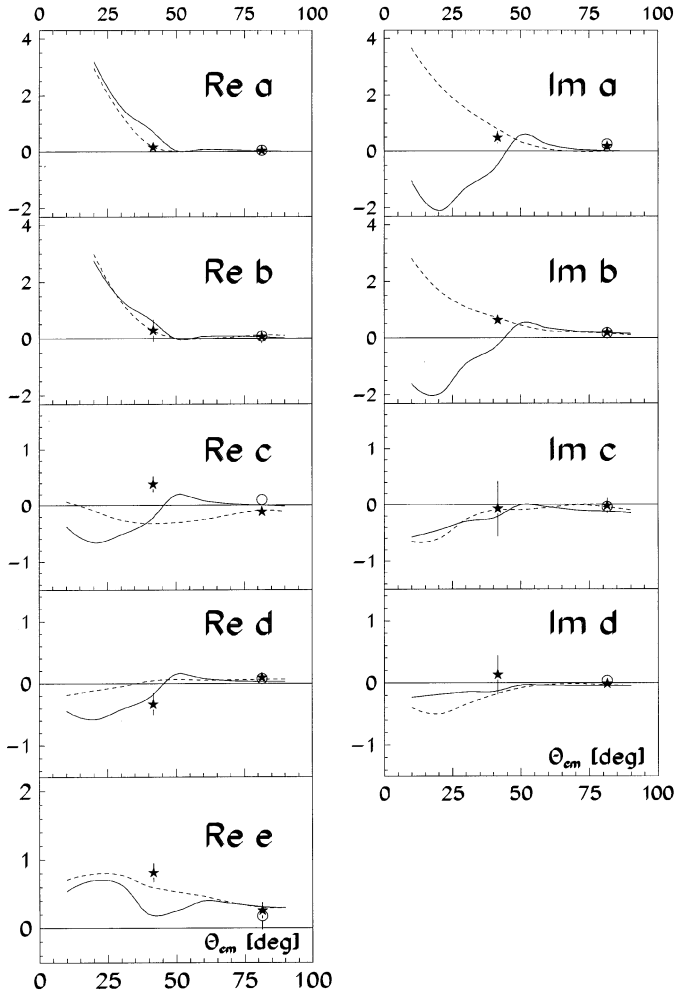


Fig. 8. Direct reconstruction of the scattering amplitudes at 2.70 GeV. Dashed and solid lines are A and B PSA solutions respectively

random initial values. The two solutions have similar χ^2 values. The total number of points, and the χ^2 values per degree of freedom (DF) of the PSA are listed in Table 1b.

For the DRSA the same database as for PSA was used. The analysis was performed at a few angles where a complete set of observables, within a small angle range exists. The experimental data for each observable were first interpolated to a common central angle. Search for solutions from random initial amplitudes was repeated several hundred times. In a few cases the solution was unique, usually 2 to 6 solutions were found. Solutions with large χ^2 values were omitted, as well as those which had very large errors on the amplitudes. In rare cases, other non-statistical criteria, which required smooth behaviour of some observable in a restrained angular interval, were used in order to reduce the number of solutions. These criteria were described in detail in [65] and will not be treated here. The comparison with PSA results was not used as a selection criterion.

Table 6. Scattering amplitudes at 2.70 GeV. The ratios of χ^2/DF are given in brackets after the solution number

Amplitude ($\sqrt{mb/sr}$)	$\theta = 41.6^\circ$ Sol. 1 (0.38)	$\theta = 81.5^\circ$ Sol. 1 (0.44)	$\theta = 81.5^\circ$ Sol. 2 (0.38)
$\Re a$	$+0.148 \pm 0.073$	$+0.030 \pm 0.014$	$+0.044 \pm 0.050$
$\Im m a$	$+0.486 \pm 0.224$	$+0.174 \pm 0.166$	$+0.254 \pm 0.132$
$\Re b$	$+0.286 \pm 0.381$	$+0.058 \pm 0.219$	$+0.083 \pm 0.115$
$\Im m b$	$+0.627 \pm 0.184$	$+0.186 \pm 0.071$	$+0.178 \pm 0.051$
$\Re c$	$+0.383 \pm 0.142$	-0.111 ± 0.039	$+0.103 \pm 0.042$
$\Im m c$	-0.070 ± 0.492	-0.019 ± 0.133	-0.039 ± 0.079
$\Re d$	-0.334 ± 0.177	$+0.091 \pm 0.038$	$+0.077 \pm 0.052$
$\Im m d$	-0.127 ± 0.312	-0.014 ± 0.063	$+0.035 \pm 0.065$
$\Re e$	$+0.813 \pm 0.140$	$+0.256 \pm 0.114$	$+0.177 \pm 0.200$

6 Results and discussion

Numerical values of the phase shifts at the four energies 1.80, 2.10, 2.40 and 2.70 GeV are given in Table 2. The phases fixed using theoretical input are also listed. The errors represent the square roots of the error matrix diagonal elements. At each energy the PSA describes existing experimental points very well as can be seen from χ^2 values in Table 1b. The energy dependence of the real and imaginary parts of phase shifts 1S_0 to 1I_6 are shown in Figs. 1 to 4 in the energy interval from 1.0 to 2.70 GeV. Open stars and open circles denote the present results, black stars and circles are our previous results from [3]. Dashed lines are OPE predictions and solid lines are the results of the Virginia Polytechnic Institute (VPI) energy-dependent PSA (SM97)[66] below 2.55 GeV. In this analysis the data from [17–19] were not yet included. Differences between the two PSA show the importance of the data lacking in [66].

Phase shifts are different in our and in VPI PSA: the singlet phase shifts (see Fig. 1) have a similar trend, the major disagreements start with the F waves. In the VPI analysis, there is no imaginary contribution coming from 3F_2 and 3H_4 phase shifts, the real part of 3F_3 and 3F_4 are totally different.

In the present PSA $\Im m ^3P_0$ has been found consistent with zero and fixed at this value at all energies except for solution B at 2.70 GeV. Because of this disagreement, it was interesting to compare the angular dependence of the scattering amplitudes, calculated by the PSA with the results of the DRSA.

The DRSA results are given in Tables 3 to 6 and are plotted in Figs. 5 to 8. The different solutions are represented by different symbols (stars, squares and circles). We see good agreement of the majority of solutions with the present PSA calculations over the entire angular interval at the three lower energies. One exception is the difference between PSA and DRSA results for $\Re c$ and $\Re d$ at 1.80 GeV below 45° CM. Note that this amplitude is small. At 2.70 GeV a DRSA was possible only at two angles. As seen in Figs. 5 to 8, amplitudes a , b and e are dominant at all energies.

The scattering amplitudes calculated by VPI PSA show a striking disagreement with the amplitudes from the

present PSA. This can be easily observed below 55 CM in $\Im m a$ and $\Im m b$. Smaller disagreements can be observed for $\Re e a$ and $\Re e b$. On the other hand, the VPI PSA agrees better with the alternate DRSA solutions at 2.10 and 2.40 GeV for $\Im m a$ and $\Im m b$. This is also true for $\Re e e$ at 1.80 and 2.10 GeV. At large angles there is a better agreement between the two PSA. One can assume that the disagreement will be reduced when all experimental points have been introduced in the VPI PSA.

7 Conclusions

A phase shift analysis and a direct amplitude reconstruction have been completed at four energies between 1.80 and 2.70 GeV. The results of the two complementary analyses agree well at all energies and give a good description of existing data points. Disagreement with the VPI PSA is likely to be due to the incomplete data base in that work. The predictions of observables will help for a planning of possible future experiments in particular at COSY.

The pp elastic differential cross sections, measured with internal proton beam during its acceleration at COSY, improve the absolute normalization at the three low energies. The present PSA show that these data need no renormalization. It is expected that the same accelerator will provide soon analyzing power and spin correlation data using a polarized internal or extracted beam and either an internal polarized proton jet-target or an external polarized target. Measurements of any observable at small angles are highly desirable in order to improve PSA and DRSA solutions below 40 CM.

Above the COSY energy limit one expects a completion of the existing pp spin-dependent database by elastic or quasielastic data measured at the JINR Dubna accelerator complex below 5 GeV. At higher energies, where the database is completely insufficient, only the KEK and BNL accelerators may provide new data in a reasonable delay.

Acknowledgements. We express our gratitude to I.I. Strakovsky for helpful discussions and for the calculations of phase shifts, amplitudes and observable predictions. One of the authors (F.L.) would like to acknowledge the support received from the University of Geneva during the period that this paper was prepared. This work was supported in part by the Swiss National Science Foundation.

References

1. J. Bystrický, C. Lechanoine-Leluc, F. Lehar, *J. Physique (Paris)* **48**, 199 (1987)
2. F. Lehar, C. Lechanoine-Leluc, J. Bystrický, *J. Physique (Paris)* **48**, 1273 (1987)
3. J. Bystrický, C. Lechanoine-Leluc and F. Lehar, *J. Phys. France* **51**, 2747 (1990)
4. F. Perrot, H. Azaiez, J. Ball, J. Bystrický, P. Chaumette, Ph. Chesny, J. Derégel, J. Fabre, J. -M. Fontaine, J. Gosset, F. Lehar, W.R. Leo, A. de Lesquen, C.R. Newsom, Y. Onel, A. Penzo, L. van Rossum, T. Siemiarczuk, J. Vrzal, C.A. Whitten and J. Yonnet, *Nucl. Phys. B* **278**, 881 (1986)
5. J. Bystrický, P. Chaumette, J. Derégel, J. Fabre, F. Lehar, A. de Lesquen, L. van Rossum, J. -M. Fontaine, J. Gosset, F. Perrot, J. Ball, T. Hasegawa, C.R. Newsom, J. Yonnet, W.R. Leo, Y. Onel, A. Penzo, H. Azaiez, A. Michalowicz, *Phys. Lett. B* **142**, 130 (1984)
6. F. Perrot, J. -M. Fontaine, F. Lehar, A. de Lesquen, J.P. Meyer, L. van Rossum, P. Chaumette, J. Derégel, J. Fabre, J. Ball, C.D. Lac, A. Michalowicz, Y. Onel, B. Aas, D. Adams, J. Bystrický, V. Ghazikhanian, G. Igo, F. Sperisen, C.A. Whitten, A. Penzo, *Nucl. Phys. B* **294**, 1001 (1987)
7. F. Lehar, A. de Lesquen, J.P. Meyer, L. van Rossum, P. Chaumette, J. Derégel, J. Fabre, J. -M. Fontaine, F. Perrot, J. Ball, C.D. Lac, A. Michalowicz, Y. Onel, D. Adams, J. Bystrický, V. Ghazikhanian, C.A. Whitten, A. Penzo, *Nucl. Phys. B* **294**, 1013 (1987)
8. F. Lehar, A. de Lesquen, L. van Rossum, J. -M. Fontaine, F. Perrot, P. Chaumette, J. Derégel, J. Fabre, J. Ball, C.D. Lac, Y. Onel, A. Michalowicz, J. Bystrický and V. Ghazikhanian, *Nucl. Phys. B* **296**, 535 (1988)
9. J. -M. Fontaine, F. Perrot, J. Bystrický, J. Derégel, F. Lehar, A. de Lesquen, L. Van Rossum, J. Ball, C.D. Lac, *Nucl. Phys. B* **321**, 299 (1989)
10. F. Perrot, J. -M. Fontaine, F. Lehar, A. de Lesquen, L. van Rossum, P. Chaumette, J. Derégel, J. Fabre, J. Ball, C.D. Lac, Y. Onel, A. Michalowicz, J. Bystrický, and V. Ghazikhanian, *Nucl. Phys. B* **296**, 527 (1988)
11. C.D. Lac, J. Ball, J. Bystrický, F. Lehar, A. de Lesquen, L. van Rossum, F. Perrot, J. -M. Fontaine, P. Chaumette, J. Derégel, J. Fabre, V. Ghazikhanian, A. Michalowicz, Y. Onel, A. Penzo, *Nucl. Phys. B* **315**, 269 (1989)
12. C.D. Lac, J. Ball, J. Bystrický, F. Lehar, A. de Lesquen, L. van Rossum, F. Perrot, J. -M. Fontaine, P. Chaumette, J. Derégel, J. Fabre, V. Ghazikhanian, A. Michalowicz, Y. Onel, A. Penzo, *Nucl. Phys. B* **315**, 284 (1989)
13. C.D. Lac, J. Ball, J. Bystrický, F. Lehar, A. de Lesquen, L. van Rossum, F. Perrot, J. -M. Fontaine, P. Chaumette, J. Derégel, J. Fabre, V. Ghazikhanian, A. Michalowicz, *Nucl. Phys. B* **321**, 269 (1989)
14. C.D. Lac, J. Ball, J. Bystrický, F. Lehar, A. de Lesquen, L. van Rossum, F. Perrot, J. -M. Fontaine, P. Chaumette, J. Derégel, J. Fabre, V. Ghazikhanian, A. Michalowicz, *Nucl. Phys. B* **321**, 284 (1989)
15. S. Dalla Torre-Colautti, R. Birsa, F. Bradamante, M. Giorgi, L. Lanceri, A. Martin, A. Penzo, P. Shavon, V. Sossi, A. Villari, H. Azaiez, K. Kuroda, A. Michalowicz, F. Lehar, *Nucl. Phys. A* **505**, 561 (1989)
16. Ch. Allgower, J. Ball, L.S. Barabash, M. Beddo, Y. Bedfer, A. Boutefnouchet, J. Bystrický, Ph. Demierre, J. -M. Fontaine, V. Ghazikhanian, D. Grosnick, R. Hess, Z. Janout, Z.F. Janout, V.A. Kalinnikov, T.E. Kasprzyk, Yu.M. Kazarinov, B.A. Khachaturov, R. Kunne, F. Lehar, A. de Lesquen, D. Lopiano, M. de Mali, V.N. Matafonov, I.L. Pisarev, A.A. Popov, A.N. Prokofiev, D. Rapin, J. -L. Sans, H.M. Spinka, S. Trentalange, Yu.A. Usov, V.V. Vikhrov, B. Vuaridel, C.A. Whitten, A.A. Zhdanov, *Eur. Phys. J. C* **1**, 131 (1998)
17. C.E. Allgower, J. Ball, M. Beddo, Y. Bedfer, A. Boutefnouchet, J. Bystrický, P. -A. Chamouard, Ph. Demierre, J. -M. Fontaine, V. Ghazikhanian, D. Grosnick, R. Hess, Z. Janout, Z.F. Janout, V.A. Kalinnikov, T.E. Kasprzyk,

- B.A. Khachaturov, R. Kunne, F. Lehar, A. de Lesquen, D. Lopiano, V.N. Matafonov, I.L. Pisarev, A.A. Popov, A.N. Prokofiev, D. Rapin, J. -L. Sans, H.M. Spinka, A. Teglia, Yu.A. Usov, V.V. Vikhrov, B. Vuaridel, C.A. Whitten and A.A. Zhdanov, Nucl. Phys. A (in press)
18. C.E. Allgower, J. Ball, L.S. Barabash, M. Beddo, Y. Bedfer, A. Boutefnouchet, J. Bystrický, P. -A. Chamouard, Ph. Demierre, J. -M. Fontaine, V. Ghazikhanian, D. Grosnick, R. Hess, Z. Janout, Z.F. Janout, V.A. Kalinnikov, T.E. Kasprzyk, Yu.M. Kazarinov, B.A. Khachaturov, R. Kunne, C. Lechanoine-LeLuc, F. Lehar, A. de Lesquen, D. Lopiano, M. de Mali, V.N. Matafonov, I.L. Pisarev, A.A. Popov, A.N. Prokofiev, D. Rapin, J. -L. Sans, H.M. Spinka, Yu.A. Usov, V.V. Vikhrov, B. Vuaridel, C.A. Whitten and A.A. Zhdanov: Eur. Phys. J. C (in press)
 19. C.E. Allgower, Ph. D thesis, Arizona State University, ANL-HEP-TR-97-71, 1997
 20. D.V. Bugg, D.C. Salter, G.H. Stafford, R.F. George, K.F. Riley, R.J. Tapper, Phys. Rev. **146**, 980 (1966)
 21. W.P. Madigan, D.A. Bell, A. Buchanan, M.M. Calkin, J.M. Clement, M. Copel, M.D. Corcoran, K.A. Johns, J.D. Lesikar, H.E. Miettinen, G.S. Mutchler, C.J. Naudet, G.P. Pepin, G.C. Phillips, J.B. Roberts, S.E. Turpin, E.V. Hungerford, B.W. Mayes, A.D. Hancock, L.S. Pinski, K.K. Sekharan, C.L. Hollas, P.J. Riley, J.C. Allred, B.E. Bonner, P. Cameron, S.T. Linn, W. von Witsch, M. Furic, V. Valkovic, Phys. Rev. D **31**, 966 (1985)
 22. Ed.K. Biegert, J.A. Buchanan, J.M. Clement, W.H. Dragoset, R.D. Felder, J.H. Hoftiezer, K.R. Hogstrom, J. Hudomalj-Gabitzsch, J.D. Lesikar, W.P. Madigan, G.S. Mutchler, G.C. Phillips, J.B. Roberts, T.M. Williams, K. Abe, R.C. Fernow, T.A. Mulera, S. Bart, B.W. Mayes and L.S. Pinski, Phys. Lett. B **73**, 235 (1978)
 23. E.F. Parker, L.G. Ratner, B.C. Brown, S.W. Gray, A.D. Krish, H.E. Miettinen, J.B. Roberts and J.R. O'Fallon, Phys. Rev. Lett. **31**, 783 (1973)
 24. I.P. Auer, E. Colton, H. Halpern, D. Hill, G. Theodosiou, D. Underwood, Y. Watanabe, and A. Yokosawa, Phys. Rev. Lett. **41**, 354 (1978)
 25. I.P. Auer, E. Colton, H. Halpern, D. Hill, R.C. Miller, H. Spinka, N. Tamura, G. Theodosiou, K. Toshioka, D. Underwood, R. Wagner, and A. Yokosawa, Phys. Rev. D **34**, 2581 (1986)
 26. R.C. Kammerud, B.B. Brabson, R.R. Crittenden, R.M. Heinz, A.H. Neal, H.W. Paik and R. Sidwell, Phys. Rev. D **4**, 1309 (1971)
 27. D.T. Williams, I.J. Bloodworth, E. Eisenhandler, W.R. Gibson, P.I.P. Kalmus, L.C.Y. Lee, Chi Kwong, G.T.J. Arnison, A. Astbury, S. Gjesdale, E. Lillethun, B. Stave, O. Ullaland, I.L. Watkins, Nuovo Cimento A **8**, 447 (1972)
 28. K.A. Jenkins, L.E. Price, F. Klem, R.J. Miller, P. Schreiner, M.L. Marshak, E.A. Peterson and K. Ruddick, Phys. Rev. D **D21**, 2445 (1980)
 29. T. Fujii, G.B. Chadwick, G.B. Collins, P.J. Duke, N.C. Hien, M.A.R. Kemp, and F. Turkot, Phys. Rev. **128**, 1836 (1962)
 30. I. Ambats, D.S. Ayres, R. Diebold, A.F. Greene, S.L. Kramer, A. Lesnik, D.R. Rust, C.E.W. Ward, A.B. Wicklund and D.D. Yovanovitch, Phys. Rev. **D9** (1974) 1179
 31. G.A. Azimov, Do In Seb, L.P. Kirilova, E.M. Kabibulina, E.N. Tsyganov, M.G. Shafranova, B.A. Shakhbazyan and A.A. Yuldashev, J. Exptl. Theor. Phys. (USSR) **42**, 340 (1962), transl. Soviet Phys. JETP **15**, 299 (1962)
 32. D. Albers, J. Bisplinghoff, R. Bollmann, K. Büßer, P. Cloth, R. Daniel, O. Diehl, F. Dohrmann, H.P. Engelhardt, J. Ernst, P.D. Eversheim, M. Gasthuber, R. Gebel, J. Greiff, A. Groß, R. Groß-Hardt, S. Heider, A. Heine, F. Hinterberger, M. Igelbrink, R. Jahn, M. Jeske, U. Lahr, R. Langkau, J. Lindlein, R. Maier, R. Maschuw, T. Mayer-Kuckuk, F. Mosel, M. Müller, F. Münstermann, D. Prasuhrn, H. Rohdjeß, D. Rosendaal, U. Roß, P. van Rossen, H. Scheid, N. Schirm, M. Schulz-Rojahn, F. Schwandt, V. Schwarz, W. Scobel, G. Sterzenbach, H.J. Trelle, A. Wellinghausen, W. Wiedmann, K. Woller, and R. Ziegler, Phys. Rev. Lett. **78**, 1652 (1997)
 33. Y. Kobayashi, K. Kobayashi, T. Nakagawa, H. Shimizu, H.Y. Yoshida, H. Ohnuma, J.A. Holt, G. Glass, J.C. Hiebert, R.A. Kenefick, S. Nath, L.C. Northcliffe, A.J. Simon, S. Hiramatsu, Y. Mori, H. Sato, A. Takagi, T. Toyama, A. Ueno, K. Imai, Nucl. Phys. A **569**, 791 (1994)
 34. J.H. Parry, N. E. Booth, G. Conforto, R.J. Esterling, J. Scheid, D.J. Sherden and A. Yokosawa, Phys. Rev. D **8**, 45 (1973)
 35. I.P. Auer, E. Colton, W.R. Dietzler, D. Hill, R. Miller, H. Spinka, G. Theodosiou, J. -J. Tavernier, N. Tamura, K. Toshioka, D. Underwood, R. Wagner, A. Yokosawa P. Kroll and W. Jauch, Phys. Rev. Lett. **51**, 1411 (1983)
 36. J. Bystrický, P. LaFrance, F. Lehar, F. Perrot, T. Siemiarczuk and P. Winternitz, J. Physique (Paris) **48**, 1901 (1987)
 37. P. Kroll, **Phenomenological Analyses of Nucleon-Nucleon Scattering**, Physics Data No. 22-1, edited by H. Behrens and G. Ebel, Fachinformationszentrum Karlsruhe 1981
 38. C. Lechanoine-Leluc and F. Lehar, Rev. Mod. Phys. **65**, 47 (1993)
 39. E. Aprile, C. Eisenegger, R. Hausammann, E. Heer, R. Hess, C. Lechanoine-LeLuc, W.R. Leo, S. Morenzoni, Y. Onel, and D. Rapin, Phys. Rev. Lett. **46**, 1047 (1981)
 40. M.W. McNaughton, S. Penttila, K.W. McNaughton, P.J. Riley, D.L. Adams, J. Bystrický, E. Gulmez and A.G. Ling, Phys. Rev. C **41**, 2809 (1990)
 41. R. Hausammann, E. Heer, R. Hess, C. Lechanoine-Leluc, W.R. Leo, Y. Onel, and D. Rapin, Phys. Rev. D **40**, 22 (1989)
 42. F. Arash, F., M.J. Moravcsik, G. Goldstein, Phys. Rev. D **32**, 74 (1985)
 43. M. Matsuda, H. Suemitsu, M. Yonezawa, Phys. Rev. D **33**, 2563 (1986)
 44. I.P. Auer, J. Chalmers, E. Colton, R. Giese, H. Halpern, D. Hill, R. Miller, K. Nield, B. Sandler, H. Spinka, N. Tamura, D. Underwood, Y. Watanabe, A. Yokosawa, A. Beretvas, and D. Miller, Phys. Rev. **D32** 1609 (1985)
 45. C.D. Lac, J. Ball, J. Bystrický, J. Derégel, F. Lehar, A. de Lesquen, L. van Rossum, J. -M. Fontaine, F. Perrot, P. Winternitz, J. Phys. France **51**, 2689 (1990)
 46. M. Lacombe, B. Loiseau, J. -M. Richard, R. Vinh Mau, J. Côté, P. Pires, and R. de Tourreil, Phys. Rev. C **21**, 861 (1980)
 47. J. Côté, M. Lacombe, B. Loiseau, and W.N. Cottingham, 1984, Nucl. Phys. A **379**, 349 (1984)
 48. B. Loiseau, J. Phys. Colloque France **46**, C-339 (1984)
 49. J. Bystrický, F. Lehar, and P. Winternitz, J. Physique (Paris) **39**, 1 (1978)
 50. S.M. Bilenky and R.M. Ryndin, Phys. Lett. **6**, 217 (1963)
 51. R.J.N. Phillips, Nucl. Phys. **43**, 413 (1963)

52. H.P. Stapp, T.J. Ypsilantis, and N. Metropolis, Phys. Rev. **105**, 302 (1957)
53. P. Cziffra, M.H. MacGregor, M.J. Moravcsik, and H.P. Stapp, Phys. Rev. **114**, 880 (1959)
54. M.H. MacGregor, M.J. Moravcsik, and H.P. Stapp, Ann. Rev. Nucl. Sci. **10**, 291 (1960)
55. N. Hoshizaki, Suppl. Prog. Theor. Phys. D **42**, 1, 107 (1968)
56. G. Breit and H. Ruppel, Phys. Rev. **127**, 2123 (1962)
57. A. Gersten, Nucl. Phys. A **290**, 445 (1977)
58. J. Bystrický, A. Gersten, A. Junod and F. Lehar, Nucl. Phys. A **285**, 469 (1976)
59. C. Lechanoine, F. Lehar, F. Perrot and P. Winternitz, Nuovo Cimento A **56**, 201 (1980)
60. R.A. Arndt, L.D. Roper, R.A. Bryan, R.B. Clark, B.J. VerWest, P. Signel, Phys. Rev. D **28**, 97 (1983)
61. R.A. Bryan, Phys. Rev. C **24**, 2659 (1981)
62. R.A. Bryan, Phys. Rev. C **30**, 305 (1984)
63. L.D. Puzikov, R.M. Ryndin and Ya.A. Smorodinskii, Nucl. Phys. **3**, 436 (1957)
64. Klepikov N.P., Zh. Eksp. Teor. Fiz. **47**, 757 (1964), transl. Sov. Phys. JETP **20**, 505 (1965)
65. J. Ball, J. Bystrický, J. -M. Fontaine, G. Gaillard, R. Hess, Z. Janout, B.A. Khachaturov, R. Kunne, C.D. Lac, C. Lechanoine-Leluc, F. Lehar, A. de Lesquen, D. Lopiano, F. Perrot-Kunne, D. Rapin, L. van Rossum, H. Schmitt and H.M. Spinka, Nuovo Cimento A **111**, 13 (1998)
66. R.A. Arndt, C.H. Oh, I.I. Strakovsky, R.L. Workman, and F. Dohrman, Phys. Rev. C **56**, 3005 (1997), SAID solution SM97